PHASE-RETARDATION EFFECTS AT RADIO FREQUENCIES IN FLAT-PLATE CONDUCTORS

D. P. BULTE[1], L. K. FORBES[2] and S. CROZIER[3]

Abstract

A system of new integral equations is presented. They are derived from Maxwell's equations and describe radio-frequency (RF) current densities on a two-dimensional flat plate. The equations are generalisations of Pocklington's integral equation showing phase-retardation in two dimensions. These singular equations are solved, numerically, for the case of one-dimensional geometry. The solutions are shown to display effects which correspond to damped resonance when the wavelength of the current matches aspects of the geometry of the conductor.

1. Introduction

In magnetic resonance imaging (MRI), the standard RF coil consists of conducting rungs placed axially along the surface of a circular cylinder, and connected at the ends by appropriate circuitry. Some designs are given in [3] and [10]. A detailed analysis of this geometry, including the effects of shielding, has been presented recently by Forbes *et al.* [7]. In addition, elliptical coil forms have also been considered by [6] in an attempt to gain better filling factors for whole-body medical imaging. In this work the mathematical techniques necessary for analysing particular types of RF coils as used in these imaging processes, and other RF applications, are developed.

Recent work [14] has indicated that bi-planar coil designs may have advantages in whole-body imaging. In a bi-planar RF coil design the primary rungs lie on two parallel planes, and the currents in the conductors on one of these planes run in the

[1]The Brain-Body Institute, St. Joseph's Healthcare, Hamilton L8N 4A6, Canada; e-mail: Daniel.Bulte@utoronto.ca.
[2]School of Mathematics and Physics, University of Tasmania, TAS 7001, Australia; e-mail: Larry.Forbes@utas.edu.au.
[3]School of Information Technology and Electrical Engineering, University of Queensland, Qld 4072, Australia; e-mail: stuart@itee.uq.edu.au.

opposite direction to the currents in the other plane. Shielding is achieved by rungs placed on an additional set of parallel planes. The analysis and optimisation of these devices is therefore of value; however, it has become evident that in order to do this a difficult problem must be overcome. This arises from the fact that a large coil experiences fully three-dimensional field effects, due to the retardation of the signal along the coil's length. The length of the coil is comparable to the wavelength of the RF signal, which consequently goes out of phase along the coil's axis.

The accurate mathematical modelling of RF coils, and their careful construction and testing, is an engineering problem of great significance in producing high-quality images of the type needed in medical applications, for example. Such imaging tools allow detailed and precise information to be developed about the internal structure of a sample, without the need for invasive techniques. It has also become important in scientific research, where it is used to image the progress of chemical reactions [9].

A method for analysing shielded bi-planar coils in the absence of retardation effects [8] has already been developed, as well as a technique for treating phase retardation effects in narrow wires [12]. Ultimately, however, the full three-dimensional retardation problem must be confronted. The present paper therefore considers the general model of radio frequency current densities in a flat conductor through the mechanism of the governing integral equations. The model is subsequently simplified to the one-dimensional case and solved to produce results which display phase-retardation effects.

2. Reduced fields for a general radiating body

When current flows in a flat plate, it is necessary to deal with the two components of the current density vector, written here as $j = e^{i\omega t}(\overline{j_x}, \overline{j_y})$, and the induced surface charge density $\sigma = e^{i\omega t}\overline{\sigma}$ [4]. The bar above the indicated variables represents the steady-state or reduced part of the quantity, after the time-harmonic part of the field has been factored out. Here, it is assumed that a sinusoidal time dependence exists throughout the region, with angular frequency ω (radians per second).

The reduced forms of Maxwell's equations are

$$\nabla \cdot \overline{D} = \overline{\rho}, \tag{2.1}$$

$$\nabla \cdot \overline{B} = 0, \tag{2.2}$$

$$\nabla \times \overline{E} = -i\omega\overline{B}, \tag{2.3}$$

$$\nabla \times \overline{H} = \overline{J} + i\omega\overline{D}, \tag{2.4}$$

in which D and E are the displacement field and the electric field, and B and H are respectively the induction and magnetic fields. The current density per area is denoted

J, while the current per length is j. Charge density per volume is represented by the symbol ρ. These may be found in the text by Ramo, Whinnery and van Duzer [13]. Now we choose to make the Lorentz gauge, and set

$$\nabla \cdot \overline{A} = -i\omega\mu\varepsilon\overline{\Phi}. \tag{2.5}$$

Scalar and vector Helmholtz equations for the scalar potential $\overline{\Phi}$ and the vector potential $\overline{A}$ may be determined. These equations are

$$\nabla^2\overline{\Phi} + \omega^2\mu\varepsilon\overline{\Phi} = -\frac{1}{\varepsilon}\overline{\rho}$$

and

$$\nabla^2\overline{A} + \omega^2\mu\varepsilon\overline{A} = -\mu\overline{J}.$$

In [12] these Helmholtz equations were solved in retarded potential form, and give rise to

$$\overline{A}(r) = \frac{\mu}{4\pi} \iiint_V \frac{e^{-i\alpha R}}{R}\overline{J}(r')\,dV', \tag{2.6}$$

$$\overline{\Phi}(r) = \frac{1}{4\pi\varepsilon} \iiint_V \frac{e^{-i\alpha R}}{R}\overline{\rho}(r')\,dV', \tag{2.7}$$

where $\alpha = \omega\sqrt{\mu\varepsilon}$ and $R = |r' - r|$. By making use of (2.6) the magnetic induction field may now be expressed by means of the formula

$$\overline{B}(r) = \frac{\mu}{4\pi} \iiint_V e^{-i\alpha R}\left(\frac{i\alpha}{R^2} + \frac{1}{R^3}\right)(r' - r) \times \overline{J}(r')\,dV'. \tag{2.8}$$

In (2.6)–(2.8), the position vector of the field point external to the conductor is denoted r, and the symbol r' represents the position of a source point within the conducting volume V.

3. Application to flat plate geometry

3.1. The magnetic induction vector   In this section, the general formula (2.8) for the magnetic induction vector is written in approximate form, appropriate to the case when the radiating body is a flat plate of negligible thickness with length L and width W. A definition sketch of the plate is given in Figure 1. The plate is assumed to be rectangular, occupying the portion $-L/2 < x < L/2$, $-W/2 < y < W/2$ of the $x - y$ plane as shown. In addition, a radio-frequency current of peak density $\bar{j}_0$
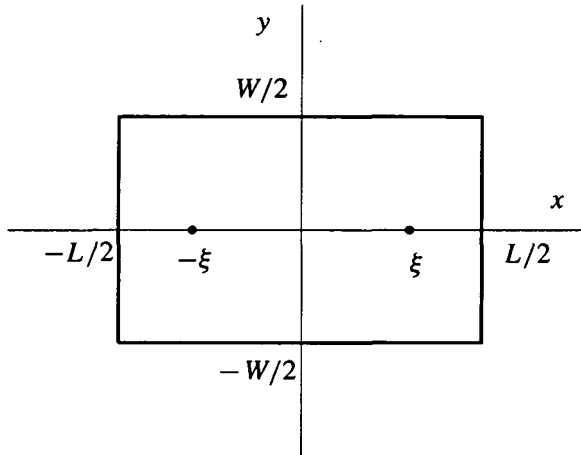
FIGURE 1. A definition sketch of the flat-plate RF radiator of length L and width W. Radio-frequency current is injected at $x = -\xi$ and extracted at $x = \xi$ as indicated.

is injected at the points $(\pm\xi, 0)$ indicated in Figure 1. (An approximate method for accounting for this current injection is described later, in Section 6.)

The boundary conditions on the surface of a perfect conductor are given, for example, in [2]. They may be written

$$n \times \overline{E} = \mathbf{0}, \tag{3.1}$$

$$n \cdot \overline{B} = 0, \tag{3.2}$$

$$n \cdot \overline{D} = \overline{\sigma}, \tag{3.3}$$

$$n \times \overline{H} = \overline{j}. \tag{3.4}$$

Because the current density vector $\overline{j}$ has the same direction on each side of the flat plate, it follows that $\overline{H}$ must be tangential to the plate, but have opposite directions on each side of it. This conclusion follows from (3.4), since the normals n are in opposite directions on each side of the plate.

If the plate has (small) thickness dh', then the volume element in the generalised Biot-Savart law (2.8) becomes $dV' = dA'dh'$, where dA' is an element of area on the plate. It follows that

$$\overline{J} = 2\frac{\overline{j}}{dh'} \tag{3.5}$$

and thus

$$\overline{J}(r')\,dV' \equiv 2\overline{j}(r')\,dA'. \tag{3.6}$$

The factor of two in (3.5) and (3.6) represents the fact that current flows on both sides of the plate. With these approximations, the induction field in (2.8) may be shown to have Cartesian components:

$$\overline{B}_x(r) = \frac{\mu}{2\pi} \iint e^{-i\alpha R} \left(\frac{i\alpha}{R^2} + \frac{1}{R^3} \right) z\overline{j}_y(r')\, dA', \tag{3.7}$$

$$\overline{B}_y(r) = -\frac{\mu}{2\pi} \iint e^{-i\alpha R} \left(\frac{i\alpha}{R^2} + \frac{1}{R^3} \right) z\overline{j}_x(r')\, dA', \tag{3.8}$$

$$\overline{B}_z(r) = \frac{\mu}{2\pi} \iint e^{-i\alpha R} \left(\frac{i\alpha}{R^2} + \frac{1}{R^3} \right) [(x' - x)\overline{j}_y(r') - (y' - y)\overline{j}_x(r')]\, dA'. \tag{3.9}$$

Allowing $z \to 0$, where $(z > 0)$, it can be shown that

$$\overline{B}_x(x, y, 0^+) = \mu\overline{j}_y(x, y, 0),$$
$$\overline{B}_y(x, y, 0^+) = -\mu\overline{j}_x(x, y, 0),$$
$$\overline{B}_z(x, y, 0^+) = 0.$$

So condition (3.4) is satisfied identically.

3.2. The electric field vector   If we now consider the electric field vector and include the solutions given in (2.6) and (2.7), then after some manipulation it can be shown that $\overline{E}$ may be expressed as

$$\overline{E}(r) = -\frac{i\omega\mu}{4\pi} \iiint_V \frac{e^{-i\alpha R}}{R} \overline{J}(r')\, dV'$$

$$- \frac{1}{4\pi\varepsilon} \iiint_V e^{-i\alpha R} \left(\frac{i\alpha}{R^2} + \frac{1}{R^3} \right) (r' - r)\overline{\rho}(r')\, dV'. \tag{3.10}$$

This expression (3.10) is appropriate to the reduced electric field produced by a body of arbitrary volume V. Once again, we now assume that V is a plate of differentially small thickness dh', from which it follows that

$$\overline{\rho}\, dV' \equiv 2\overline{\sigma}\, dA'. \tag{3.11}$$

As before, the factor of two in (3.11) represents the fact that charge density $\overline{\sigma}$ (Coulombs per square metre) is present on both sides of the plate, and dA' is the element of area. The plate itself lies on the plane $z' = 0$, and the three Cartesian

components of (3.10) therefore become

$$
\overline{E_x}(r) = -\frac{i\omega\mu}{2\pi} \iint \frac{e^{-i\alpha R}}{R} \overline{j_x}(r')\, dA'
$$
$$
- \frac{1}{2\pi\varepsilon} \iint e^{-i\alpha R} \left(\frac{i\alpha}{R^2} + \frac{1}{R^3}\right)(x' - x)\overline{\sigma}(r')\, dA', \qquad (3.12)
$$
$$
\overline{E_y}(r) = -\frac{i\omega\mu}{2\pi} \iint \frac{e^{-i\alpha R}}{R} \overline{j_y}(r')\, dA'
$$
$$
- \frac{1}{2\pi\varepsilon} \iint e^{-i\alpha R} \left(\frac{i\alpha}{R^2} + \frac{1}{R^3}\right)(y' - y)\overline{\sigma}(r')\, dA', \qquad (3.13)
$$
$$
\overline{E_z}(r) = -\frac{i\omega\mu}{2\pi} \iint \frac{e^{-i\alpha R}}{R} \overline{j_z}(r')\, dA'
$$
$$
- \frac{1}{2\pi\varepsilon} \iint e^{-i\alpha R} \left(\frac{i\alpha}{R^2} + \frac{1}{R^3}\right)(-z)\overline{\sigma}(r')\, dA'. \qquad (3.14)
$$

Now take the limit $z \to 0$ for $(z > 0)$ and consider the component $\overline{E_z}$. We have $\overline{j_z} \equiv 0$, and so

$$
\overline{E_z}(x, y, z) = \frac{z}{2\pi\varepsilon} \int_{-L/2}^{L/2} \int_{-W/2}^{W/2} e^{-i\alpha R} \left[\frac{i\alpha}{(x' - x)^2 + (y' - y)^2 + z^2} \right.
$$
$$
\left. + \frac{1}{[(x' - x)^2 + (y' - y)^2 + z^2]^{3/2}} \right] \overline{\sigma}(x', y')\, dy'\, dx'.
$$

Using this result, and (3.12) and (3.13), it may now be shown that, as $z \to 0$,

$$
\overline{E_x}(x, y, 0^+) = 0,
$$
$$
\overline{E_y}(x, y, 0^+) = 0,
$$
$$
\overline{E_z}(x, y, 0^+) = \overline{\sigma}(x, y)/\varepsilon.
$$

It is evident from these results that boundary condition (3.3) is satisfied identically.

4. The integral equations for a flat plate

The retarded-potential solutions in Sections 3.1 and 3.2 satisfy the field equations (2.1)–(2.4), but it remains to satisfy boundary conditions (3.1)–(3.4) completely. We show in this section that this leads to a system of three integral equations for the two components $\overline{j_x}$ and $\overline{j_y}$ of the current density vector, and the charge density $\overline{\sigma}$, on the plate.

Boundary conditions (3.2) and (3.4) are satisfied if the condition

$$\int_{-L/2}^{L/2} \int_{-W/2}^{W/2} e^{-i\omega R_0} \left(\frac{i\alpha}{R_0^2} + \frac{1}{R_0^3} \right) [(x' - x)\overline{j_y}(r') - (y' - y)\overline{j_x}(r')] \, dy' \, dx' = 0 \quad (4.1)$$

is obeyed. Similarly, the full satisfaction of boundary conditions (3.1) and (3.3) requires that

$$i\omega\mu\varepsilon \int_{-L/2}^{L/2} \int_{-W/2}^{W/2} \frac{e^{-i\omega R_0}}{R_0} \overline{j_x}(r') \, dy' \, dx'$$
$$+ \int_{-L/2}^{L/2} \int_{-W/2}^{W/2} e^{-i\omega R_0} \left(\frac{i\alpha}{R_0^2} + \frac{1}{R_0^3} \right) (x' - x)\overline{\sigma}(r') \, dy' \, dx' = 0 \quad (4.2)$$

and

$$i\omega\mu\varepsilon \int_{-L/2}^{L/2} \int_{-W/2}^{W/2} \frac{e^{-i\omega R_0}}{R_0} \overline{j_y}(r') \, dy' \, dx'$$
$$+ \int_{-L/2}^{L/2} \int_{-W/2}^{W/2} e^{-i\omega R_0} \left(\frac{i\alpha}{R_0^2} + \frac{1}{R_0^3} \right) (y' - y)\overline{\sigma}(r') \, dy' \, dx' = 0, \quad (4.3)$$

where $R_0 = \sqrt{(x' - x)^2 + (y' - y)^2}$ and $\alpha = \omega\sqrt{\mu\varepsilon}$.

Equations (4.1) to (4.3) are therefore the integral equations that determine the current-density components $\overline{j_x}$ and $\overline{j_y}$ and the charge density $\overline{\sigma}$. They are evidently a generalisation of Pocklington's (and Hallen's) integral equations as given in Balanis [2].

Experience shows that it is extremely difficult to solve this system numerically, and numerical experiments suggest that only two of these three equations (4.1)–(4.3) are actually independent. Thus it appears that one of the three equations is linearly dependent on the other two, although we have not so far been able to prove this in the full two-dimensional case. The system is made more difficult to solve by the fact that the unknown functions are all complex quantities. A simpler, related problem, arising in airfoil theory, was solved by Tuck [15] using a Galerkin method. However, he dealt with a single equation of this type, which only involved real quantities.

5. Reduction to one-dimensional geometry

In view of the difficulty in solving the full two-dimensional system of equations, we concentrate here on the simpler problem of seeking a solution in one dimension only. This yields insights into the structure of the solutions. The reduced current density components $\overline{j_x}$ and $\overline{j_y}$ and the charge density $\overline{\sigma}$ are assumed to depend on x alone, which corresponds to a plate of infinite width ($W \to \infty$).

Under these conditions (4.1), (4.2) and (4.3) reduce to

$$\pi\alpha^2 \int_{-L/2}^{L/2} (x' - x)\overline{j_y}(x') F_1(\alpha|x' - x|) \, dx' = 0, \tag{5.1}$$

$$i\omega\mu\varepsilon(-\pi i) \int_{-L/2}^{L/2} \overline{j_x}(x') H_0^{(2)}(\alpha|x' - x|) \, dx'$$

$$+ \pi\alpha^2 \int_{-L/2}^{L/2} (x' - x)\overline{\sigma}(x') F_1(\alpha|x' - x|) \, dx' = 0 \tag{5.2}$$

and

$$i\omega\mu\varepsilon(-\pi i) \int_{-L/2}^{L/2} \overline{j_y}(x') H_0^{(2)}(\alpha|x' - x|) \, dx' = 0. \tag{5.3}$$

Here $H_0^{(2)}(\psi)$ is the Hankel function of order zero, and of the second kind [11], and it is convenient to define the auxiliary function

$$F_1(z) = \frac{2}{\pi} \int_0^{\infty} e^{-iz\cosh\psi} \left[\frac{i}{z\cosh\psi} + \frac{1}{z^2\cosh^2\psi} \right] d\psi. \tag{5.4}$$

Once again, it is found that (5.1) is linearly dependent on (5.2) and (5.3). Equation (5.3) has only the trivial solution $\overline{j_y}(x) = 0$, and therefore only (5.2) remains for the range of non-trivial solutions.

5.1. The continuity equation
Although there are three integral equations (5.1)–(5.3) for the three unknowns $\overline{j_x}$, $\overline{j_y}$ and $\overline{\sigma}$, only two of them are independent, and so some extra information is needed. This is provided by means of the continuity equation [2], which may be written

$$\iiint_V \frac{\partial\rho}{\partial t} \, dV' + \oiint_S J \cdot n \, dS' = 0. \tag{5.5}$$

Equation (5.5) can be written in a form appropriate to a flat plate, using (3.5), (3.6) and (3.11). The result [10] is

$$\frac{\partial\sigma}{\partial t} + \frac{\partial j_x}{\partial x} + \frac{\partial j_y}{\partial y} = 0. \tag{5.6}$$

In the present one-dimensional case $\overline{j_y} = 0$ and in reduced variables (5.6) becomes

$$i\omega\overline{\sigma} + \frac{\partial\overline{j_x}}{\partial x} = 0.$$

Combining this result with (5.2) produces

$$\int_{-L/2}^{L/2} \overline{j_x}(x') H_0^{(2)}(\alpha|x' - x|) \, dx' + i \int_{-L/2}^{L/2} \frac{\partial\overline{j_x}}{\partial x'}(x' - x) F_1(\alpha|x' - x|) \, dx' = 0. \tag{5.7}$$

This is a singular, integrodifferential equation for $\overline{j_x}(x)$. Obviously, one solution is the trivial case $\overline{j_x} \equiv 0$. This is as expected, since if there is no input/output current, then only the trivial case is relevant. However, we are concerned with the non-trivial case, and so input and output voltage terms must be included explicitly.

6. The numerical method

This section presents a numerical method for obtaining solutions to the governing integral equation (5.7), in the one-dimensional approximation. In this case, the injected RF current is accounted for by means of an overall (reduced) current density of magnitude $\overline{j_0}$ inserted at the point $x = -\xi$ and extracted at the point $x = \xi$. This is a width-averaged approximation to the situation shown in Figure 1, appropriate to the one-dimensional case considered here.

As indicated in Sections 4 and 5, extensive numerical experience has shown that the governing system of equations is highly ill-conditioned (this has been confirmed both in the one-dimensional and two-dimensional cases). Accordingly, the numerical solution technique we have chosen in this paper avoids excessive sophistication, and opts instead for the robustness of a straightforward low-order method. A solution was selected in a basis-function expansion of the form

$$\overline{j_x}(x) = \sum_{n=1}^{N} A_n \psi_n(x), \qquad -L/2 < x < -\xi, \; \xi < x < L/2,$$

$$\overline{j_x}(x) = \overline{j_0} + \sum_{n=1}^{N} A_n \psi_n(x), \qquad -\xi < x < \xi,$$

and so it follows that

$$\frac{\partial j_x}{\partial x} = \sum_{n=1}^{N} A_n \psi_n'(x), \qquad -L/2 < x < L/2. \tag{6.1}$$

The basis functions were required to be symmetrical about the origin (the centre of the plate), and free to take any value at the edges of the plate, and therefore the chosen functions were $\psi_n = \cos(n\pi x/L)$. Now the integrodifferential equation (5.7) becomes

$$\int_{-\xi}^{\xi} \overline{j_0} H_0^{(2)}(\alpha|x' - x|)\, dx' + \sum_{n=1}^{N} A_n \int_{-L/2}^{L/2} \psi_n(x') H_0^{(2)}(\alpha|x' - x|)\, dx'$$

$$+ i \sum_{n=1}^{N} A_n \int_{-L/2}^{L/2} \psi_n'(x')(x' - x) F_1(\alpha|x' - x|)\, dx' \approx 0.$$

We now set up a mesh of N numerical grid points at

$$x_k = (k - 1)\Delta x, \quad (k = 1, 2, \ldots, N),$$

over half of the plate ($0 < x < L/2$), with equal point spacing given by

$$\Delta x = \frac{L}{2(N - 1)}.$$

Evaluating the integral equation at the $(N-1)$ interior mesh points x_k ($k=1, \ldots, N-1$) produces the system

$$\sum_{n=1}^{N} T_{kn} A_n \approx R_k, \quad (k = 1, 2, \ldots, N - 1), \tag{6.2}$$

where

$$T_{kn} = \int_{-L/2}^{L/2} dx' \{\psi_n(x') H_0^{(2)}(\alpha|x' - x_k|) + i\psi_n'(x')(x' - x_k) F_1(\alpha|x' - x_k|)\}$$

and

$$R_k = -\overline{j_0} \int_{-\xi}^{\xi} H_0^{(2)}(\alpha|x' - x_k|) \, dx'.$$

6.1. Dealing with singularities Difficulties arise in evaluating the terms T_{kn} and R_k in (6.2) because these involve singular integrals. The integrals involving the Hankel functions may be rendered non-singular by using the identity

$$\int_{-M}^{M} f(x') H_0^{(2)}(\alpha|x' - x_k|) \, dx'$$
$$= \int_{-M}^{M} \left[f(x') H_0^{(2)}(\alpha|x' - x_k|) - \frac{2}{\pi i} f(x_k) \ln(\alpha|x' - x_k|) \right] dx'$$
$$+ \frac{2f(x_k)}{\pi i} [2M(\ln\alpha - 1) + (M - x_k) \ln|M - x_k| + (M + x_k) \ln|M + x_k|].$$

This result comes from subtraction of the singular part of the Hankel function (see [1]). The integrals involving the F_1 terms have Cauchy-type singularities in the one-dimensional case. Therefore employing the Cauchy principal value interpretation (avoiding the case where $x' \equiv x_k$) produces the non-singular form

$$\text{CPV} \int_{-M}^{M} f(x')(x' - x_k) F_1(\alpha|x' - x_k|) \, dx'$$
$$= \int_{-M}^{M} \left[f(x')(x' - x_k) F_1(\alpha|x' - x_k|) - \frac{2}{\pi\alpha^2} f(x_k) \frac{1}{x' - x_k} \right] dx'$$
$$+ \frac{2}{\pi\alpha^2} f(x_k) \ln\left(\frac{M - x_k}{M + x_k}\right).$$
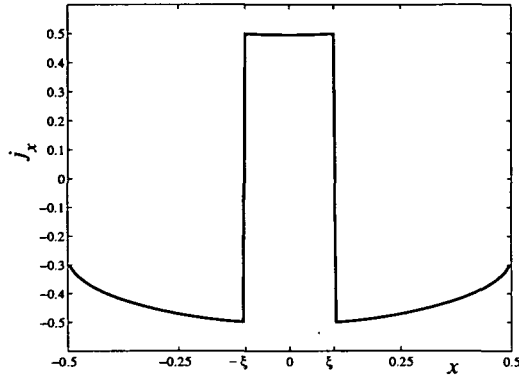
FIGURE 2. Current waveform along plate, $\xi = 0.1$ m, $\omega = 1.0 \times 10^9$ rad.s^{-1} and $L = 1.0$ m. Here $N = 201$.
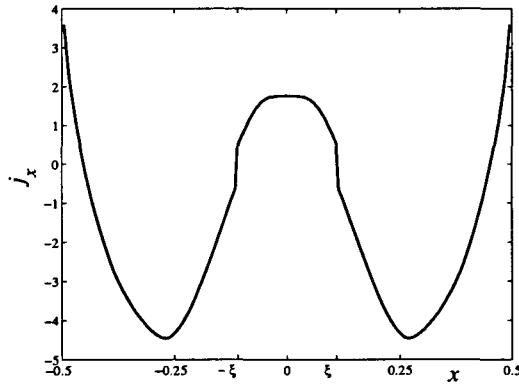
FIGURE 3. Current waveform along plate $\xi = 0.11$ m, $\omega = 4.0 \times 10^9$ rad.s^{-1} and $L = 1.0$ m. Here $N = 201$.

These integrals may now be evaluated using almost any quadrature rule, and we employ the trapezoidal rule, typically using $\sim$ 200 points to preserve numerical accuracy. The exact derivation of these equations is shown in Appendix A.

7. The current solutions

The one-dimensional model in Section 5 was first solved for frequencies close to those which have applications in MRI, as this was the situation which provided the impetus for the investigation. Figure 2 shows the solution waveform of j_x along the plate at a frequency of $\omega = 1.0 \times 10^9$ rad.s^{-1}. The solution shown is a snap shot at time $t = 0$. The discontinuity at $\pm\xi$ is caused by the insertion and extraction
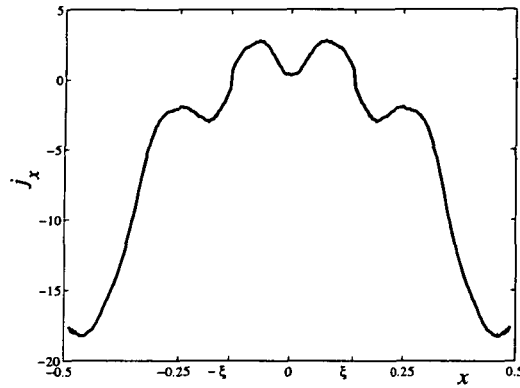
FIGURE 4. Solution at a configuration which produces resonance. Horizontal axis: position on plate, Vertical axis: current amplitude, $\xi = 0.14\,\text{m}$, $\omega = 4.0 \times 10^9\,\text{rad.s}^{-1}$ and $L = 1.0\,\text{m}$. Here $N = 305$.
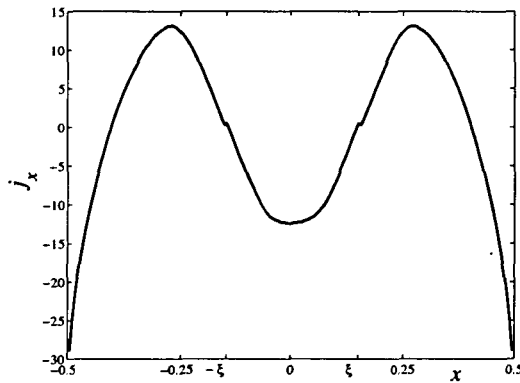
FIGURE 5. Waveform showing inversion: $\xi = 0.15\,\text{m}$, $\omega = 4.0 \times 10^9\,\text{rad.s}^{-1}$ and $L = 1.0\,\text{m}$. Here $N = 201$.

of the current on the plate at those two points. In Figure 3 the frequency ω is $4.0 \times 10^9\,\text{rad.s}^{-1}$, the length of the plate is 1 m and the distance from the origin to the current insertion/extraction is 0.11 m. The amplitude of the current density j_0 is arbitrarily set at $1\,\text{Am}^{-1}$.

The wavelength of radiation appropriate to this frequency is approximately 0.47 m. This is consistent with the result shown in Figure 3, since the separation of the two troughs in this diagram has about this value. This confirms the reliability of the numerical scheme outlined in Section 6.

7.1. Damped resonance   Numerical experiments were carried out, in which the length L of the plate was fixed, but the separation distance 2ξ between the current in-

jection/extraction points was varied (at constant angular frequency ω). It was observed that, for ξ larger than a certain value, the waveform "inverted", so that the solution profile gave the appearance of having been multiplied by some negative constant. The behaviour is consistent with resonance, since the amplitude of the waveform increased as the critical separation length ξ was approached, and the waveform inverted at values of ξ larger than this critical value. However, the resonance behaviour is damped, since arbitrarily large amplitudes could not be observed in the wave profiles, and there was a continuous transition between a solution and its "inverted" form, in a narrow band of values of ξ near the resonant value. An example of an inverted waveform is given in Figure 5. Figures 3–5 show this continuous transition.

It is evident that this phenomenon is associated with resonance, since the critical separation distance 2ξ at which it occurs is close to half the free wavelength of radiation at the given frequency. This value depends on the plate length L and the frequency ω.

8. Conclusions

New integral equations (2.6) and (2.7) have been derived from Maxwell's equations which describe in full the electric field and induction vectors for radio frequency signals emitted from a flat plate. This system of equations was reduced to one dimension and solved for a number of different configurations to demonstrate its robustness. The solution for the full two-dimensional system will be presented in a future article.

The solutions presented show the significance of phase-retardation effects in these circumstances. In an MRI full-body scan the RF coils can include rungs up to 1 m in length and carry currents at comparable frequencies to those dealt with here. The differences between current densities and fields calculated without considering phase retardation can be significant.

It has been shown in this work that damped resonance behaviour can occur, and this is an extreme case of the effects of phase retardation in these systems. Although these resonances have been revealed only from the numerical solution of a difficult mathematical equation, they can nevertheless be understood in terms of the physics of the situation. The resonances occur when the separation distance 2ξ is roughly comparable to half the free wavelength of radiation at this frequency, but they are damped because the flat plate radiates energy away to infinity. As is standard for damped resonances, the precise resonant frequency is altered somewhat by the strength of the effective damping term, but this is difficult to determine in this complicated system.

The more difficult case of radiation from a fully two-dimensional plate, for which the integral equations are presented in Section 4, has not been discussed in this paper. It clearly could involve much more complicated resonant behaviour, and will be

discussed in a future article.

Acknowledgements

Appendix A.

In order to render the integrals in (6.2) non-singular the singular part is removed by subtraction, and integrated explicitly. In the case of the Hankel function $H_0^{(2)}(\alpha|x' - x_k|)$, there is a a logarithmic singularity as $x' \to x_k$ [1]. Thus

$$H_0^{(2)}(\alpha|x' - x_k|) \to \frac{2}{\pi i} \ln(\alpha|x' - x_k|),$$

as $x' \to x_k$. Therefore, to evaluate integrals of the form

$$\int_{-M}^{M} f(x') H_0^{(2)}(\alpha|x' - x_k|) \, dx'$$

using numerical quadrature, we express them as

$$
\begin{aligned}
\int_{-M}^{M} &\left[f(x') H_0^{(2)}(\alpha|x' - x_k|) - f(x_k) \frac{2}{\pi i} \ln(\alpha|x' - x_k|) \right] dx' \\
&+ f(x_k) \frac{2}{\pi i} \int_{-M}^{M} \ln(\alpha|x' - x_k|) \, dx' \\
&= \int_{-M}^{M} \left[f(x') H_0^{(2)}(\alpha|x' - x_k|) - \frac{2}{\pi i} f(x_k) \ln(\alpha|x' - x_k|) \right] dx' \\
&+ \frac{2f(x_k)}{\pi i} [2M(\ln \alpha - 1) + (M - x_k) \ln|M - x_k| + (M + x_k) \ln|M + x_k|].
\end{aligned}
$$

The term in the integral in this last expression is zero if $x' = x_k$; thus the integral is now non-singular and may be integrated quite simply.

For integrals of the form

$$\int_{-M}^{M} f(x')(x' - x_k) F_1(\alpha|x' - x_k|) \, dx', \qquad (A.1)$$

it is necessary to consider $F_1(k)$ in the limit $k \to 0$. From (5.4), this function may be written

$$F_1(k) = \frac{2}{\pi k^2} \int_0^{\infty} e^{-ik \cosh \psi} \left[\frac{ik}{\cosh \psi} + \frac{1}{\cosh^2 \psi} \right] d\psi.$$

Allowing $k \to 0$ in the integrand of this expression gives

$$F_1(k) \to \frac{2}{\pi k^2}[1 - 0].$$

It follows that

$$(x' - x_k) F_1(\alpha|x' - x_k|) \to \frac{2}{\pi \alpha^2} \frac{1}{x' - x_k}, \quad \text{as } x' \to x_k.$$

Therefore the integral in (A.1) has a Cauchy-type singularity (in one dimension). Thus the integral may be interpreted in the Cauchy principal value sense, and so

$$\text{CPV} \int_{-M}^{M} f(x')(x' - x_k) F_1(\alpha|x' - x_k|) \, dx'$$

$$= \int_{-M}^{M} \left[f(x')(x' - x_k) F_1(\alpha|x' - x_k|) - f(x_k) \frac{2}{\pi \alpha^2 (x' - x_k)} \right] dx'$$

$$+ \frac{2}{\pi \alpha^2} f(x_k) \text{CPV} \int_{-M}^{M} \frac{dx'}{x' - x_k}.$$

However,

$$\text{CPV} \int_{-M}^{M} \frac{dx'}{x' - x_k} = \ln\left(\frac{M - x_k}{M + x_k}\right).$$

Thus the Cauchy principal value interpretation gives

$$\text{CPV} \int_{-M}^{M} f(x')(x' - x_k) F_1(\alpha|x' - x_k| \, dx'$$

$$= \int_{-M}^{M} \left[f(x')(x' - x_k) F_1(\alpha|x' - x_k|) - \frac{2}{\pi \alpha^2} f(x_k) \frac{1}{x' - x_k} \right] dx'$$

$$+ \frac{2}{\pi \alpha^2} f(x_k) \ln\left(\frac{M - x_k}{M + x_k}\right),$$

which is non-singular and so may be integrated easily, avoiding the case where $x' \equiv x_k$.

References

[1] M. Abramowitz and I. A. Stegun, *Handbook of functions with formulas, graphs and mathematical tables* (Dover, New York, 1972).
[2] C. Balanis, *Advanced engineering eletromagnetics* (John Wiley & Sons, New York, 1989).
[3] P. Callaghan, *Principles of nuclear magnetic resonance microscopy* (Oxford Scientific Publications, Oxford, 1993).

[4] D. Cheng, *Fundamentals of engineering electromagnetics* (Addison-Wesley World Student Series, San Francisco, 1992).

[5] L. K. Forbes, S. Crozier and D. M. Doddrell, "Determining current distributions for RF resonators in magnetic resonance imaging", *Meas. Sci. Technol.* **6** (1995) 284–292.

[6] L. K. Forbes, S. Crozier and D. M. Doddrell, "An analysis and optimization of elliptical RF probes used in magnetic resonance imaging", *Meas. Sci. Technol.* **7** (1996) 1281–1290.

[7] L. K. Forbes, S. Crozier and D. M. Doddrell, "Calculating current densities and fields produced by shielded magnetic resonance imaging probes", *SIAM J. Appl. Math.* **57** (1997) 401–425.

[8] L. K. Forbes, S. Crozier and D. M. Doddrell, "Calculating current densities and fields due to shielded bi-planar radio-frequency coils", *Meas. Sci. Technol.* **9** (1998) 1609–1619.

[9] L. F. Gladden, "Nuclear magnetic resonance in chemical engineering: principles and applications", *Chem. Eng. Sci.* **49** (1994) 3339–3408.

[10] J. Jin, *Electromagnetic analysis and design in magnetic resonance imaging* (CRC Press, Boca Raton, 1999).

[11] E. Kreyszig, *Advanced engineering mathematics*, 6th ed. (John Wiley & Sons, New York, 1988).

[12] C. Mahoney, L. K. Forbes, S. Crozier and D. M. Doddrell, "A novel approach to the calculation of RF magnetic and electric fields for NMR coils of arbitrary geometry", *J. Magn. Reson. Ser. B* **107** (1995) 145–151.

[13] S. Ramo, J. R. Whinnery and T. Van Duzer, *Fields and waves in communication electronics* (John Wiley & Sons, New York, 1965).

[14] D. Roberts, E. Insko, L. Bolinger and J. Leigh Jr., "Biplanar radio frequency coil design", *J. Magn. Reson. Ser. A* **102** (1993) 34–41.

[15] E. O. Tuck, "Some accurate solutions of the lifting surface integral equation", *J. Austral. Math. Soc. Ser. B* **35** (1993) 127–144.